Quasi-IMAT Study with Conventional Equipment to Show High Plan Quality with a Single Gantry Arc

Judith Alvarez Moret, Oliver Kölbl, Ludwig Bogner[1]

Background and Purpose: Nowadays, intensity-modulated arc therapy (IMAT) for clinical use is mostly based on forward planning. The aim of this work is to investigate the potential of a step-and-shoot quasi-IMAT (qIMAT) technique to improve plan quality.
Material and Method: qIMAT plans with 18 and 36 beams were generated with a total number of 36 segments. Additionally, the number of segments was increased to 72, in order to investigate if the quality of the plans improves with the number of beams and segments. A conventional six-field intensity-modulated radiation therapy (IMRT) plan was used as a reference. The beam setup was applied to the CarPet phantom and to five prostate cancer patients.
Results: In the phantom case, the dose received by the organ at risk (OAR) decreased considerably by using qIMAT. At the same time, coverage and homogeneity of planning target volume (PTV) remained unaffected. For the prostate cases, a good dose coverage was accomplished inside the PTV. Rectum and bladder were better spared with qIMAT. When increasing the number of segments, only a slight improvement of the plan quality was observed.
Conclusion: The study showed that qIMAT improves the sparing of OARs while keeping the uniformity within the PTV, when compared with conventional IMRT. The more concave the PTV, the more noticeable is this behavior. The qIMAT technique has the advantage that it can be realized with a conventional equipment. The plan quality is high even with a single gantry arc and one segment per beam direction.

Key Words: IMAT · Tomotherapy · VMAT

Strahlenther Onkol 2009;185:41–48
DOI 10.1007/s00066-009-1890-2

Quasi-IMAT-Studie zur Untersuchung der Planqualität mit einer einzigen Gantryrotation mit konventioneller Ausrüstung

Hintergrund und Ziel: Die klinische Anwendung der intensitätsmodulierten Arc-Therapie (IMAT) erfolgt derzeit hauptsächlich durch Vorwärtsplanung. Das Ziel dieser Studie ist, das Potential einer „step-and-shoot"-Quasi-IMAT-(qIMAT-)Technik zur Erhöhung der Planqualität zu untersuchen.
Material und Methodik: qIMAT-Pläne mit 18 und 36 Feldern und maximal 36 Segmenten wurden erzeugt. Zusätzlich wurde die Segmentzahl auf 72 erhöht, um eine potentielle Verbesserung in Abhängigkeit von der Felder- und Segmentzahl zu untersuchen. Ein konventioneller IMRT-Plan (intensitätsmodulierte Strahlentherapie) mit sechs Feldern wurde als Referenz benutzt. Die Konfiguration der Felder wurde am CarPet-Phantom und an fünf Prostatakrebsfällen angewendet.
Ergebnisse: Beim Phantom nahm die deponierte Dosis im Risikoorgan (OAR) deutlich ab, wenn qIMAT angewendet wurde. Gleichzeitig blieben die Abdeckung des Zielvolumens und Homogenität des Planungszielvolumens (PTV) unverändert. Bei den Prostatafällen konnte eine gute Abdeckung des Zielvolumens erreicht werden. Rektum und Blase wurden mit qIMAT besser geschont. Bei Erhöhung der Segmentzahl wurde eine leichte Verbesserung beobachtet.
Schlussfolgerung: Die Untersuchung zeigte, dass qIMAT weniger Dosis im OAR deponierte, während die Homogenität im PTV im Vergleich zur konventionellen IMRT gleich blieb. Dieses Verhalten wird ausgeprägter, wenn der Grad der Konkavität des PTVs zunimmt. Der Vorteil der qIMAT-Methode besteht darin, dass eine Verbesserung der Planqualität mit konventioneller Ausrüstung erreicht werden kann. Die Planqualität ist bereits mit einer Quasirotation bei einem Segment pro Einstrahlrichtung hoch.

Schlüsselwörter: IMAT · Tomotherapie · VMAT

[1]Department of Radiotherapy, University of Regensburg, Germany.

Received: April 21, 2008; accepted: October 31, 2008

Introduction

Intensity-modulated arc therapy (IMAT) [8, 14, 19, 24, 25] was proposed by Yu [25] as an alternative to tomotherapy [2, 7, 12, 15, 18, 22]. Both techniques are rotational approaches to intensity-modulated radiation therapy (IMRT), and they are able to improve the therapeutic ratio [6, 11, 21]. Helical tomotherapy delivers the dose slice by slice with a binary multileaf collimator (MLC) that modulates the intensity while the source rotates around the patient. The patient is moved translationally such yielding a helical delivery. Otherwise, IMAT can be delivered by overlapping several arcs while continuously shaping the field form or simultaneously modulating the intensity and the gantry speed with a dynamic MLC [17].

All these attempts to realize IMAT can be grouped into [19]:

(a) forward aperture-based segmentation, the only available technique which is implemented in clinical use. Some investigators have described an approach using various arc paths [14]. This approach can achieve high-quality plans but it cannot be applied to all tumor sizes and locations [10, 16].
(b) leaf-sequencing: optimized intensity patterns are determined for each beam angle. Next, a leaf-sequencing algorithm translates each intensity pattern into a set of deliverable aperture shapes. This method requires a large number of arcs, with the consequence of a long delivery time [25].
(c) direct aperture optimization (DAO), a recently presented method with no leaf-sequencing requirement [9, 20]. DAO optimizes the shapes and the weights of the apertures directly, without previous fluence optimization. Applied to step and shoot, IMRT is capable to create conformal plans. However, its application to IMAT has not yet been successful, because the IMAT constraints make it more difficult to find an optimal solution [9]. The application of DAO to IMAT is very promising.

The aim of this study is to investigate an inversely planned quasi-IMAT (qIMAT) technique by applying a large number of fields in step-and-shoot IMRT technique. This method offers many advantages such as the use of a conventional treatment-planning system (TPS) and linear accelerator. It is especially interesting to investigate if the plan quality can be improved with comparable delivery time, when compared to a six-field reference plan.

Material and Methods

CarPet Phantom and Patients: Structure Definition

A CT image set of the anthropomorphic pelvic-like CarPet phantom (Quasimodo IMRT verification project, Figure 1) was used for this study [3]. It contains four structures: planning target volume (PTV; drawn in 52 slices with a thickness of 2 mm) that surrounds a circular organ at risk (OAR), body contour without the PTV (body-PTV), and a help contour to avoid hot spots. In the longitudinal direction an anterior-posterior shift is applied to the respective contours by 0.25 cm/cm distance. We consider this phantom an extreme case of prostate cancer.

Five patients with localized prostate cancer were included in the study. All patients had three-dimensional CT images with a slice thickness of 5 mm. Five structures were defined: PTV, OARs (rectum and bladder), and two help contours. Although we chose patients with similar structures, there were small differences in terms of rectum and bladder overlap with PTV and also concerning PTV concavity between the five cases. Three of the five patients had no seminal vesicle involvement and, therefore, a low concavity. The two cases with seminal vesicle involvement presented a medium degree of concavity.

Equipment and Radiation Technique

Treatment planning was performed with the TPS Oncentra Masterplan® v3.0 (Nucletron BV, Veenendaal, The Netherlands). The option direct step and shoot (DSS) [1, 13] was used for the optimization process. In this option the user can define a maximum total number of segments to be used. A fluence optimization with subsequent leaf sequencing is performed for a few iterations to get an initial guess for the segments. Afterwards, the gradients of the objective function are calculated with respect to leaf positions and weights and MLC segments are optimized directly. The number of segments is reduced by elimination of segments with similar shape. The result of the optimization is a set of MLC segments ready for delivery without further postprocessing. A more detailed description can be found in [13].

The plans were created on a Siemens Primus linear accelerator with a photon energy of 15 MV and an MLC with 29 leaf pairs with 1 cm leaf width at the isocenter for the 27 inner leaf pairs and 6.5 cm for the two outer leaf pairs.

For the CarPet phantom as well as for the patient cases, two qIMAT plans (with 18 and 36 beam directions: qIMAT18 and qIMAT36) were generated in order to simulate a rota-

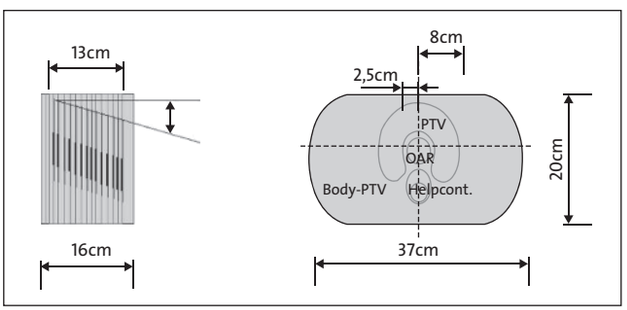

Figure 1. Sagittal and transverse views of the CarPet phantom and its structures. PTV and OAR are shifted vertically from slice to slice (angle Φ).

Abbildung 1. Darstellung einer Sagittal- und Transversalebene des CarPet-Phantoms und seiner Strukturen. PTV und OAR sind von Schicht zu Schicht vertikal verschoben (Winkel Φ).

tional technique. A conventional six-field plan was also created as a reference plan. The gantry angles were equidistant, except for the reference plan for the patient cases. For these cases, a usual set of beam orientations for prostate cancer was used: 25°, 90°, 120°, 240°, 270°, and 335°. For dose calculation the pencil-beam algorithm was used with a dose grid resolution of 0.4 cm. The minimal number of open leaf pairs was set to two and the minimal open field size was set to 4 cm^2. The minimal number of monitor units per fraction and per segment was set to one.

In order to investigate if the plan quality and the number of segments are correlated by a fixed number of beams, two versions (with a total number of 36 and 72 segments) were performed for each plan.

Treatment Goals

The dose-volume objectives (DVOs) and constraints used during the optimization process for the CarPet phantom are listed in Table 1. For the prostate cancer cases, another set of DVOs listed in Table 2 was used.

Each optimization was performed with a target dose of 60 Gy to the PTV to be delivered in 30 fractions. All plans were normalized to have the same average dose into the PTV (60 Gy).

Evaluation

The evaluation was performed in terms of dose-volume histograms (DVHs) and dose statistics for the PTVs and OARs. The phantom plans were evaluated by means of the DVOs described in the ESTRO's study [3]: PTV: $V_{95} \geq 99\%$ and $V_{105} < 5\%$; OAR: $V_{70} < 1\%$ and body-PTV (unspecified tissue outside the target volume): $V_{80} < 15\%$, $V_{100} < 2\%$, $D_{max} < 105\%$. In addition, the DVH points D_{99}, D_1, and homogeneity of PTV were also considered. For the prostate cancer cases, the set of DVH points selected for the evaluation is listed in Table 4.

A Wilcoxon test was performed with the statistical software SPSS v15.0 (SPSS Inc., Chicago, IL, USA) for a statistical analysis of the data. For a p-value < 0.05, the difference was considered significant. Standard deviation is reported as well.

Due to the large number of beams of the qIMAT plans, an important parameter to investigate was the delivery time. For this purpose, the most extreme treatment plans with six and 36 fields (both optimized with 36 segments) corresponding to the phantom were delivered and the delivery times for a fraction of 200 cGy are also given.

Results

DVH Analysis and Dose Distributions

Quasimodo: Concave Target Volume

Results of the study corresponding to the DVHs of the CarPet phantom are reported in Table 3. When comparing the reference plan with qIMAT36, having the maximum number of segments set at 36, qIMAT left the homogeneity of the dose distribution within PTV nearly unchanged at about 12%. Simultaneously, the averaged dose received by the OAR decreased considerably from 42.8 Gy to 32.5 Gy and V_{70} from 60.7% to 21.7%. The average dose received by the normal tissue decreased significantly (from 25.4 Gy to 19.7 Gy). The number of monitor units was similar in all cases. By increasing the number of segments to 72, no significant improvement concerning dose sparing was observed. However, the PTV coverage V_{95} improved in all cases and the monitor units increased significantly by applying qIMAT.

The DVH (Figure 2) with comparison of the three plans (corresponding to the scheme with 36 segments) showed, that the larger the number of beam directions, the lower the dose

Table 1. Constraints and dose-volume objectives (DVOs) used for optimization of the CarPet phantom. The reason for the choice of such a high weight for the volume body-PTV was that in the treatment-planning system a violation of a DVO for a small volume (OAR) has a larger impact on the objective function than for a large volume. D: dose (expressed in Gy); OAR: organ at risk; PTV: planning target volume; W: weight.

Tabelle 1. Dosis-Volumen-Randbedingungen, die beim Optimierungsprozess am CarPet-Phantom benutzt wurden. Der Grund für ein so hohes Gewicht der Außenkontur abzüglich PTV (Body-PTV) ist, dass in Oncentra Masterplan® die Überschreitung eines DVOs bei einem kleinen Volumen (OAR) eine niedrigere Wirkung hat als bei einem großen Volumen. D: Dosis (in Gy); OAR: Risikoorgan; PTV: Planungszielvolumen; W: Gewicht.

PTV D_{max}	PTV D_{min}	OAR D_{40}	W	OAR D_{max}	W	Body-PTV D_{30}	W	Body-PTV D_{max}	W	Help contour D_{40}	W	Help contour D_{max}	W
62	59	40	2,000	42	1,000	30	5,000	50	6,000	40	1,000	45	1,500

Table 2. Constraints and dose-volume objectives used for optimization of the prostate cancer cases. OARs: organs at risk (i.e., rectum and bladder); W: weight.

Tabelle 2. Constraint- und Dose-Volume-Objective-(DVO-)Werte, die beim Optimierungsprozess der Prostatafälle benutzt wurden. OARs: Risikoorgane (d.h. Rektum und Blase); W: Gewicht.

PTV D_{max} (Gy)	PTV D_{min} (Gy)	OARs D_{20} (Gy)	W	OARs D_{max} (Gy)	W	Help structure D_{max} (Gy)	W
64	59	40	2,500	59	3,000	40	1,500

Table 3. Comparison of plan quality for the CarPet phantom resulting from the optimization: V_{95}, V_{105}, V_{70}, V_{80}, V_{100} (partial volumes receiving > 95%, 105%, 70%, 80%, and 100% of the prescribed dose); D_1 and D_{99} (the 1st and the 99th percentile dose); homogeneity factor H, defined as $(D_5–D_{95})*100/D_{av.}$ (D_5 and D_{95} are the doses encompassing 5% and 95% of the planning target volume [PTV] and $D_{av.}$ is the average dose in the PTV). The lower H, the more homogeneous is the dose. #B: number of beams; MU: monitor units; OAR: organ at risk; #S: number of segments.

Tabelle 3. Vergleich verschiedener Dosis-Volumen-Randbedingungen für die drei verschiedenen Phantompläne: V_{95}, V_{105}, V_{70}, V_{80}, V_{100} (Teil des Volumens, das > 95%, 105%, 70%, 80% und 100% der Solldosis erhält); D_1 und D_{99} (1. und 99. Perzentilendosis); Homogenitätsfaktor H, definiert als $(D_5–D_{95})*100/D_{av.}$ (D_5 und D_{95} sind die Dosiswerte, die 5% und 95% des Planungszielvolumens erhalten, und $D_{av.}$ ist der Dosismittelwert im PTV). Je kleiner H, desto homogener ist die Dosis. #B: Anzahl der Felder: MU: Monitoreinheiten; OAR: Risikoorgan; #S: Anzahl der Segmente.

#B	#S	MU	PTV					OAR		Body-PTV				Help contour
			D_{99} (Gy)	D_1 (Gy)	H (%)	V_{95} (%)	V_{105} (%)	$D_{av.}$ (Gy)	V_{70} (%)	$D_{av.}$ (Gy)	V_{80} (%)	V_{100} (%)	D_{max} (%)	D_{av} (Gy)
6	36	475.6	54.0	64.7	12.5	90.0	8.0	42.8	60.7	25.4	9.9	0.3	108.9	40.4
18	36	465.6	54.2	64.2	10.0	93.7	3.4	37.6	31.0	23.4	13.9	0.7	111.1	29.2
36	36	465.4	53.7	63.7	12.0	88.0	3.9	32.5	21.7	19.7	10.2	1.0	108.5	22.2
6	70	513.0	54.3	64.5	11.7	91.5	6.4	43.3	62.7	25.5	10.0	0.1	105.4	40.5
18	72	799.2	55.6	63.8	9.7	94.6	3.0	35.1	9.8	23.8	8.6	0.1	106.6	36.2
36	68	625.1	55.2	63.2	9.5	93.2	1.7	34.4	16.3	22.4	8.9	0.1	104.0	21.1

received by the OAR and normal tissue was. The differences in the PTV were not significant. A comparison of the dose distributions generated for the three plans in a transverse slice is shown in Figure 3. The distributions of the dose showed that the isodose lines were more conform to the PTV, if a large number of beams were used.

Prostate Cases

Results of the study for the five patients are summarized in Table 4 as average values. The selected DVH points corresponding to the qIMAT plans were compared with the reference plan. The comparison was performed for the two plan types with 36 and 72 segments.

Having the maximum number of segments set at 36, the plan quality improved by using qIMAT, when compared to the reference plan. Although the homogeneity of the dose distribution within the PTV did not change significantly from reference plan to qIMAT36 (25.8% vs. 26.7%; $p = 0.50$), the OARs were better spared: $D_{80,rectum}$ decreased from 34.7% to 24.1% ($p = 0.07$), $D_{50,rectum}$ from 54.4% to 50.7% ($p = 0.50$), and $D_{50,bladder}$ from 45.0% to 41.7% ($p = 0.23$). The number of monitor units increased significantly by using 18 beam directions, but did not significantly change by using 36.

Increasing the number of segments (such allowing DSS to use a maximum of 72 segments), the homogeneity of the dose within the PTV increased significantly from 24.9% to 23.5% (reference plan and qIMAT36; $p < 0.05$). Rectal dose sparing expressed by D_{50} increased with the number of beams: from 54.5% (six fields) to 50.4% (18 fields; $p < 0.05$) up to 48.9% (36 fields; $p = 0.08$). These values were similar to the values corresponding to the 36-segment scheme. The behavior of the bladder presented no dependence on the number of beam directions. A decrease of average dose deposited in the rectum was observed in both cases by using qIMAT: from 34.0 Gy to 33.0 Gy down to 31.0 Gy (with $p = 0.23$ and $p < 0.05$, respectively, by using 36 segments) and from 34.0 Gy to 32.4 Gy down to 30.5 Gy (with $p < 0.05$ and $p < 0.05$, respectively, by using 72 segments). It was observed that in the cases with medium concavity, the dose sparing to OARs increased more than in the cases with low PTV concavity, when applying qIMAT.

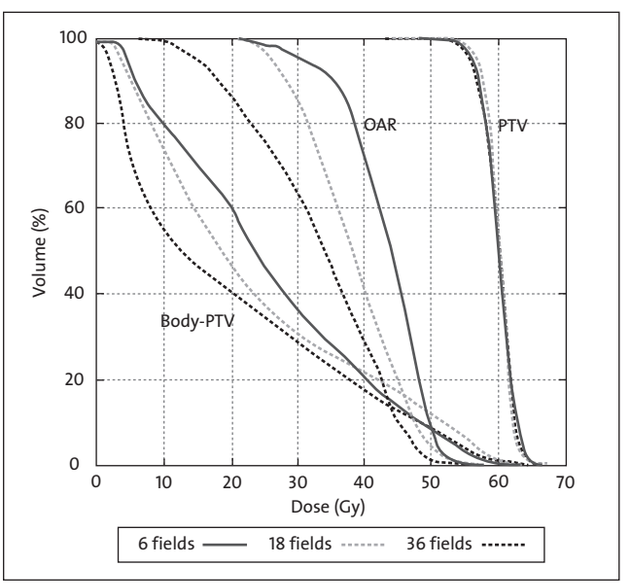

Figure 2. DVH comparison of the reference plan with the qIMAT plans applied to the CarPet phantom by using 36 segments.

Abbildung 2. Vergleich der DVHs des Referenzplans mit den qIMAT-Plänen für das Phantom.

Delivery Time

The plans used to investigate the delivery time had 475.6 MU (six fields) and 464.4 MU (qIMAT36). The times to deliver

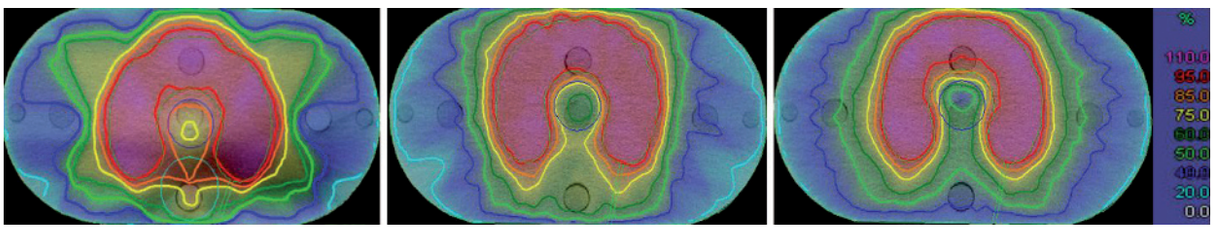

Figure 3. Dose distributions for the CarPet phantom when 36 segments were used. The 20%, 40%, 50%, 60%, 75%, 85%, 95%, and 110% isodose lines are shown on each plot.

Abbildung 3. Dosisverteilungen für das CarPet-Phantom bei Verwendung von 36 Segmenten. Dargestellt sind die 20%-, 40%-, 50%-, 60%-, 75%-, 85%-, 95%- und 110%-Isodosenlinien.

Table 4. Comparison of plan quality for the patient cases resulting from optimization (averaged values for five patients). Evaluated DVH points: D_{80}, D_{50} and D_5 for the organs at risk (i.e., bladder and rectum), D_{99}, D_1 (minimal and maximal doses) and homogeneity for planning target volume (PTV). Standard deviation and p-values comparing qIMAT18 and qIMAT36 with reference plan are also given. MU: monitor units; qIMAT: quasi-intensity-modulated arc therapy.

Tabelle 4. Vergleich verschiedener Parameter für die fünf Patienten (Mittelwerte): D_{80}, D_{50} und D_5 für die Risikoorgane (Blase und Rektum), D_{99}, D_1 (minimale und maximale Dosis) und Homogenität der Dosis im Planungszielvolumen (PTV). Standardabweichungen und p-Werte, die den Referenzplan mit qIMAT18 und qIMAT36 vergleichen, sind ebenfalls angegeben. MU: Monitoreinheiten; qIMAT: quasi-intensitätsmodulierte Arc-Therapie.

		Six fields	qIMAT18	qIMAT36	p-value (6/18)	p-value (6/36)
36 segments	Total MU	461.7 ± 29.4	620.4 ± 90.0	493.9 ± 127.8	0.04	0.69
	PTV					
	D_{99} (%) ± σ	84.6 ± 2.0	85.3 ± 2.9	84.5 ± 2.5	0.14	0.69
	D_1 (%) ± σ	107.3 ± 1.1	107.3 ± 1.0	108.1 ± 1.2	0.89	0.10
	H	25.8 ± 3.7	24.5 ± 3.9	26.7 ± 3.8	0.08	0.50
	Rectum					
	$D_{av.}$ (%) ± σ	34.0 ± 5.8	33.0 ± 4.8	31.0 ± 4.2	0.23	0.04
	D_{80} (%) ± σ	34.7 ± 17.2	31.8 ± 15.7	24.1 ± 13.3	0.23	0.07
	D_{50} (%) ± σ	54.4 ± 7.1	53.3 ± 3.6	50.7 ± 4.1	0.08	0.50
	D_5 (%) ± σ	98.4 ± 1.7	97.8 ± 2.7	98.1 ± 2.2	0.50	0.08
	Bladder					
	$D_{av.}$ (%) ± σ	32.1 ± 9.3	32.6 ± 8.9	31.3 ± 8.5	0.23	0.23
	D_{50} (%) ± σ	45.0 ± 21.8	44.2 ± 20.4	41.7 ± 19.1	0.23	0.23
	D_5 (%) ± σ	100.4 ± 1.9	101.3 ± 2.5	100.8 ± 2.1	0.07	0.11
	Total MU	527.0 ± 20.4	642.3 ± 68.2	706.7 ± 112.5	0.08	0.04
72 segments	**PTV**					
	D_{99} (%) ± σ	85.0 ± 2.1	86.1 ± 2.3	85.5 ± 2.7	0.04	0.23
	D_1 (%) ± σ	106.5 ± 0.7	106.6 ± 0.5	107.0 ± 0.7	0.89	0.04
	H	24.9 ± 3.9	22.6 ± 3.4	23.5 ± 3.7	0.04	0.04
	Rectum					
	$D_{av.}$ (%) ± σ	34.0 ± 5.5	32.4 ± 4.8	30.5 ± 5.7	0.04	0.04
	D_{80} (%) ± σ	34.0 ± 16.9	28.6 ± 14.1	24.0 ± 12.7	0.04	0.04
	D_{50} (%) ± σ	54.5 ± 5.8	50.4 ± 4.2	48.9 ± 1.6	0.04	0.08
	D_5 (%) ± σ	99.0 ± 1.9	99.1 ± 1.6	97.8 ± 2.8	0.72	0.07
	Bladder					
	$D_{av.}$ (%) ± σ	32.1 ± 9.1	32.0 ± 8.5	32.1 ± 8.7	0.47	0.89
	D_{50} (%) ± σ	44.3 ± 21.4	42.8 ± 19.6	43.1 ± 19.9	0.22	0.50
	D_5 (%) ± σ	100.1 ± 1.9	101.0 ± 1.9	101.3 ± 2.6	0.07	0.07

these monitor units were 9 min for the reference plan and 12 min for the qIMAT36. The Siemens Primus linac applies the IM-MAXX™ option if more than one segment per beam is delivered. This option shuts down the accelerator gun only during rotation of the gantry from one beam angle to the next, but from segment to segment within a beam it is only deflected.

Discussion

In terms of OAR sparing, qIMAT improved the plan quality in all cases, particularly in the case of the CarPet phantom. All phantom plans showed acceptable PTV coverage and homogeneity. The six-field reference plan could not spare dose to the OAR as efficiently as the qIMAT plans. Comparing the maximum dose received by the PTV, the lowest values cor-

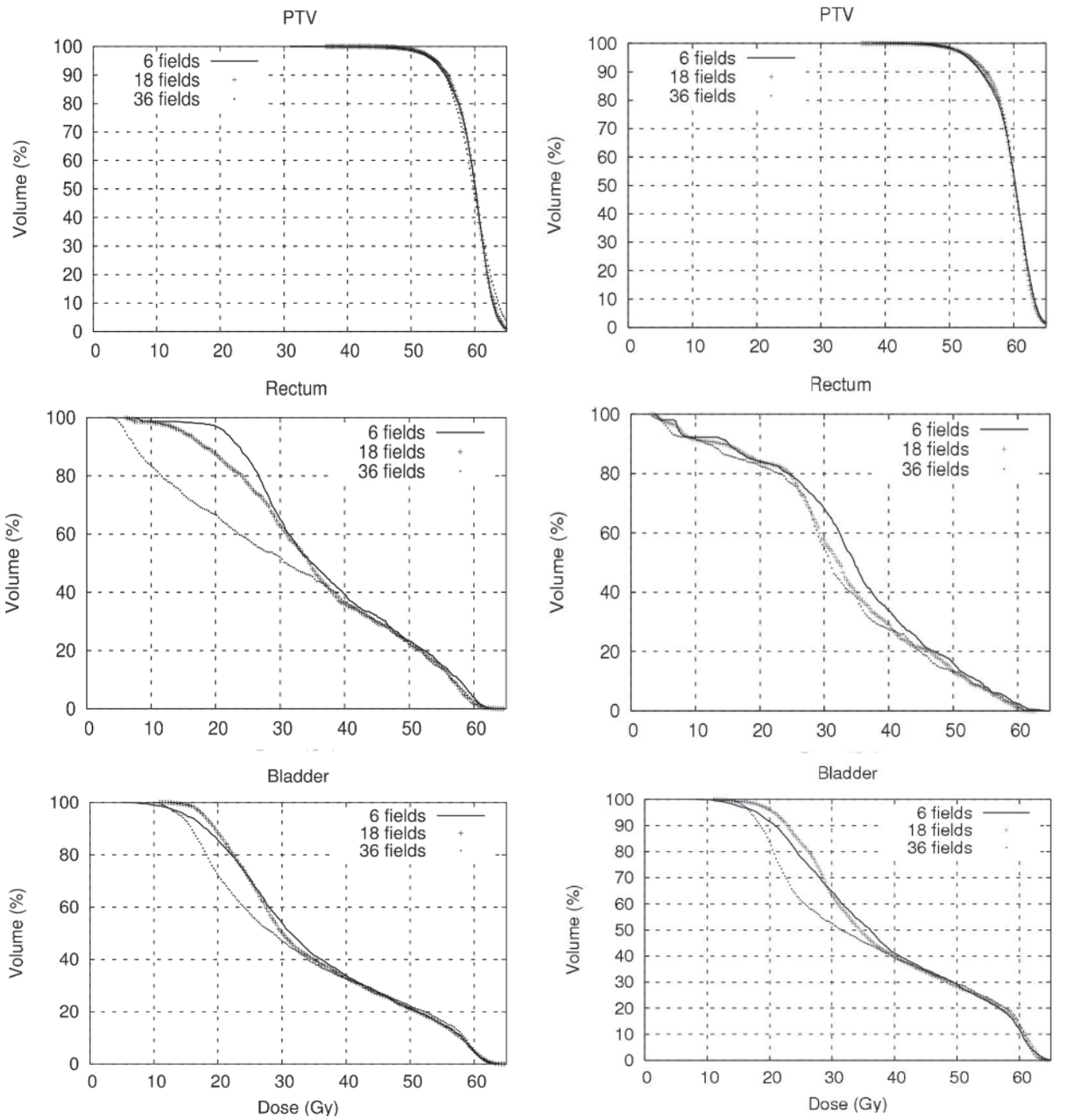

Figures 4a and 4b. DVHs corresponding to two typical cases of prostate cancer. a) Patient with medium PTV concavity. b) Patient with low PTV concavity.

Abbildungen 4a und 4b. DVHs zweier typischer Prostatakrebspläne. a) Patient mit konkavem PTV. b) Patient mit wenig konkavem PTV.

responded to the qIMAT technique. The use of qIMAT led to a considerable reduction of the mean dose received by the normal tissue and, consequently, by the OAR while keeping similar or even better PTV coverage compared to conventional IMRT.

Concerning the planning study with five prostate cancer patients, the DVH analysis (Figure 4) showed that the dose received by the OARs was lower in all cases when applying the qIMAT technique, although these differences were not always similarly significant. The dose coverage of the PTV for the three plans was quite similar by using 36 segments but significantly improved ($p < 0.05$) when increasing the number of segments to 72. Compared to the reference plan, the qIMAT plans significantly increased the total number of monitor units in all cases, except for the qIMAT36 plan with 36 segments (corresponding to one single rotation around the patient).

When comparing the qIMAT dose distributions with the reference plan, the isodose lines were highly conformal to the PTV for the qIMAT plans.

In both parts of the study, an improvement of the plan quality was observed by using qIMAT. However, the results also showed that the degree of improvement depends on the concavity of the PTV. qIMAT plans, which have a large number of beam directions, were capable of a more conformal dose delivery to the concave PTV and a better dose sparing of the central OAR than the reference plan. This could especially be observed in the phantom, that has an extremely concave and large PTV. The prostate cancer cases presented different degrees of improvement with qIMAT. qIMAT led to a considerable improvement in the two cases with high concavity, but was comparable to the reference plan in the other three patients. This is a conclusion drawn also by other authors who used the CarPet phantom or other markedly concave PTV structures for their investigations [4, 5].

An important issue was the time of treatment delivery. Although the plans had similar monitor units, for the qIMAT36 plan the gantry has to be changed every 10°. This fact can increase the time of treatment delivery. The reference plan was delivered within 9 min. The time for qIMAT36 was longer (12 min) in comparison to the reference plan. The accelerator used the IM-MAXX™ option when more than one segment per beam is delivered. This option speeds up treatment delivery of IMRT plans by maintaining the radiation beam "on" while delivering segments at a defined angle. The factor of time reduction by using this option could be estimated to be approximately 0.75. Taking this factor into account, the delivery time of the qIMAT plan would decrease from 12 to approximately 9 min, if this option would be available.

Conclusion

Shepard et al. [19] discussed different approaches to IMAT. To our knowledge, up to now no clinical application of inversely planned IMAT has been done. Only forward planned IMAT techniques are in clinical use. An important advantage over dynamic methods is that an improvement of the plan quality can be achieved with a standard IMRT TPS and a standard linac equipment without any option for dynamic delivery. The improvement of the plan quality depends on the degree of concavity of the PTV. Cases with high concavity benefit from this method. By using 36 beam directions and one segment per direction (simulation of a single gantry arc rotation), the plan quality is even high. Despite the large number of beam directions, the delivery time was comparable to the six-field IMRT. Dynamic beam delivery should reduce treatment time considerably [17], but at the price of the necessity to dispose of a specialized equipment. A study to determine if the risk of developing secondary cancers after qIMAT radiation differs from that associated with conventional IMRT is currently under way [23].

Acknowledgment

This work was supported by Elekta AB.

References

1. Ahnesjo A, Hardermark B, Isacsson U, et al. The IMRT information process-mastering the degrees of freedom in external beam therapy. Phys Med Biol 2006;51:R381–402.
2. Beavis AW. Is tomotherapy the future of IMRT? Br J Radiol 2004;77: 285–95.
3. Bohsung J, Gillis S, Arrans R, et al. IMRT treatment planning – a comparative inter-system and intercentre planning exercice of the ESTRO QUASIMODO Group. Radiother Oncol 2005;76:354–61.
4. Bratengeier K. Applications of two-step intensity modulated arc therapy. Strahlenther Onkol 2001;177:394–403.
5. Bratengeier K, Guckenberger M, Meyer J, et al. A comparison between 2-step IMRT and conventional IMRT planning, Radiother Oncol 2007;84: 298–306.
6. Cao D, Holmes T, Afghan M, et al. Comparison of plan quality provided by intensity-modulated arc therapy and helical tomotherapy. Int J Radiat Oncol Biol Phys 2007;69:240–50.
7. Carol M, Grant WH 3rd, Pavord D, et al. Initial clinical experience with the Peacock intensity modulation of a 3-D conformal radiation therapy system. Stereotact Funct Neurosurg 1996;66:30–4.
8. Duthoy W, De Gersem W, Vergote K, et al. Clinical implementation of intensity-modulated arc therapy (IMAT) for rectal cancer. Int J Radiat Oncol Biol Phys 2004;60:794–806.
9. Earl MA, Shepard DM, Naqvi S, et al. Inverse planning for intensity-modulated arc therapy using direct aperture optimization. Phys Med Biol 2003;48:1075–89.
10. Edlund T, Zimmer JR, Gannett DE. IMRT for the treatment of prostate cancer: a comparison of a forward-planned technique and an inverse-planned technique utilizing a dose gradient method. Med Dosim 2004;29:128–33.
11. Fiorino C, Dell'Oca I, Pierelli A, et al. Significant improvement in normal tissue sparing and target coverage for head and neck cancer by means of helical tomotherapy. Radiother Oncol 2006;78:276-82.
12. Fiorino C, Dell'Oca I, Pierelli A, et al. Simultaneous integrated boost (SIB) for nasopharynx cancer with helical tomotherapy. A planning study.. Strahlenther Onkol 2007;183:497–505.
13. Hardemark B, Liander A, Rehbinder H, et al. Direct machine parameter optimization with RayMachine in Pinnacle. RaySearch White Paper. RaySearch Laboratories AB, Stockholm, Sweden: 2003.
14. Ma L, Yu CX, Earl M, et al. Optimized intensity-modulated arc therapy for prostate cancer treatment. Int J Cancer 2001;96:379–84.
15. Mackie TR, Holmes T, Swerdloff S, et al. Tomotherapy: a new concept for the delivery of dynamic conformal radiotherapy. Med Phys 1993;20:1709–19.
16. Mihai A, Rakovitch E, Sixel K, et al. Inverse vs forward breast IMRT planning. Med Dosim 2005;30:149–54.

17. Otto K. Volumetric modulated arc therapy: IMRT in a single gantry arc. Med Phys 2008;35:310–7.
18. Rochet N, Sterzing F, Jensen A, et al. Helical tomotherapy as a new treatment technique for whole abdominal irradiation. Strahlenther Onkol 2008;184:145–9.
19. Shepard DM, Cao D, Afghan MK, et al. An arc-sequencing algorithm for intensity modulated arc therapy. Med Phys 2007;34:464–70.
20. Shepard DM, Earl MA, Li XA, et al. Direct aperture optimization: a turnkey solution for step-and-shoot IMRT. Med Phys 2002;29:1007–18.
21. Sterzing F, Schubert K, Sroka-Perez G, et al. Helical tomotherapy. Experiences of the first 150 patients in Heidelberg. Strahlenther Onkol 2008;184:8–14.
22. Welsh S, Patel RR, Ritter MA, et al. Helical tomotherapy: an innovative technology and approach to radiation therapy. Technol Cancer Res Treat 2002;1:311–6.
23. Wiezorek T, Voigt A, Metzger N, et al. Experimental determination of peripheral doses for different IMRT techniques delivered by a Siemens linear accelerator. Strahlenther Onkol 2008;184:73–9.
24. Wong E, Chen JZ, Greenland J, et al. Intensity-modulated arc therapy simplified. Int J Radiat Oncol Biol Phys 2003;53:222–35.
25. Yu CX. Intensity-modulated arc therapy with dynamic multileaf collimation: an alternative to tomotherapy. Phys Med Biol 1995;40:1435–49.

Address for Correspondence
Judith Alvarez Moret
Department of Radiotherapy
University of Regensburg
Franz-Josef-Strauß-Allee 11
93053 Regensburg
Germany
Phone (+49/941) 944-7630, Fax -7612
e-mail: judith.alvarez-moret@klinik.uni-regensburg.de